

On the Elastic Properties and Fracture Patterns of MoX_2 ($X = \text{S}, \text{Se}, \text{Te}$) Membranes: A Reactive Molecular Dynamics Study

M. L. Pereira Júnior^a, C. M. Viana de Araújo^a, J. M. de Sousa^b, R. T. de Sousa Júnior^c, L. F. Roncaratti Júnior^a, W. F. Giozza^c and L. A. Ribeiro Júnior^{a,*}

^a*Institute of Physics, University of Brasília, Brasília, 70910-900, Brazil.*

^b*Federal Institute of Education, Science and Technology of Piauí, São Raimundo Nonato, Piauí, Brazil.*

^c*Department of Electrical Engineering, University of Brasília 70919-970, Brazil.*

ARTICLE INFO

Keywords:

Transition Metal Dichalcogenides
Molybdenum-based TMDs
Elastic Properties
Fracture Patterns
Reactive Molecular Dynamics

ABSTRACT

We carried out fully-atomistic reactive molecular dynamics simulations to study the elastic properties and fracture patterns of transition metal dichalcogenide (TMD) MoX_2 ($X=\text{S},\text{Se},\text{Te}$) membranes, in their 2H and 1T phases, within the framework of the Stillinger-Weber potential. Results showed that the fracture mechanism of these membranes occurs through a fast crack propagation followed by their abrupt rupture into moieties. As a general trend, the translated arrangement of the chalcogen atoms in the 1T phase contributes to diminishing their structural stability when contrasted with the 2H one. Among the TMDs studied here, 2H- MoSe_2 has higher tensile strength (25.98 GPa).

1. Introduction

Transition metal dichalcogenide (TMD) monolayers are atomically thin semiconductors that belong to the family of 2D nanosheets [1, 2]. They present an MX_2 arrangement, where M is a transition metal, and X is a chalcogen. The combination of chalcogen (e.g., S, Se, or Te) and transition metal atoms (typically Mo, W, Nb, Re, Ni, or V) yields more than 40 different materials [3, 4]. Each monolayer has a thickness of 6 – 7 Å and is hexagonally-packed by transition metal atoms sandwiched between two layers of chalcogen atoms [3]. TMDs are graphene cognate and possible to synthesize by applying the same chemical methods usually employed in producing the latter [5, 6]. These materials have received much attention in the fields of biomedicine [7, 8], optoelectronics [9, 10], and energy conversion and storage [11, 12]. Particularly, MoS_2 and MoTe_2 monolayers — direct bandgap semiconductors with bandgaps about 1.9 eV [13] and 1.0 eV [14], respectively — have emerged as promising candidates in replacing gapless graphene to develop novel applications in which semiconducting materials are desired [15]. MoSe_2 , in turn, is an indirect bandgap semiconductor (with a bandgap about 1.58 eV [16]) that has also been widely employed in developing new applications in flat electronics [17, 18]. To further explore the potential of these TMDs species in boosting new advances in the research fields mentioned above, their mechanical properties should be deeply understood.

TMD nanostructures have three different structural arrangements, named 2H, 1T, and 1T' [19]. 2H and 1T refer to the hexagonal and trigonal structures, respectively. The 1T' phase is a distorted form of 1T. Significant theoretical and

✉ ribeirojr@unb.br (L.A.R. Júnior)
ORCID(s):

experimental efforts have been employed in understanding the mechanical properties of layered MoS₂ [20–34], MoSe₂ [35–38], and MoTe₂ [39–45] on both 2H and 1T forms. In these investigations, it was experimentally studied few layers (5-25) of these TMDs species, and Young's modulus obtain were approximately 330 Gpa [21], 117 Gpa [38], and 110 Gpa [43] for MoS₂, MoSe₂, and MoTe₂, respectively. By using density functional theory and reactive molecular dynamic simulations, theoretical studies have predicted Yong's modulus values for single-layer MoS₂, MoSe₂, and MoTe₂ ranging in the intervals 170-250 Gpa [20, 24, 33], 165-185 Gpa [46, 47], and 60-115 Gpa [41, 44, 45], respectively. These works promoted substantial advances in understanding the mechanical properties of TMDs. However, an overall description of their elastic properties and fracture dynamics is still missing.

Herein, we carried out extensive fully-atomistic reactive molecular dynamics simulations to study the elastic properties and fracture dynamics of MoX₂ (X=S,Se,Te) membranes in their 2H and 1T phases. The elastic properties were obtained from the stress-strain relationship. Only recently, 1T phases of these materials were experimentally realized [19]. In this sense, a detailed description of the mechanical properties of these nanostructures considering both 2H and 1T phases is highly attractive.

2. Methodology

We performed fully-atomistic molecular dynamics (MD) simulations using the Stillinger-Weber (SW) [25, 26] potential as implemented by LAMMPS [48]. Figure 1 illustrates the model TMDs monolayers studied here in their 2H and 1T phases. The left, middle, and bottom panes illustrate the MoS₂, MoSe₂, and MoTe₂ monolayers, respectively, in the H (top panels) and T phases (bottom panels). Their atomistic structure contains 3456, 3348, and 2688 atoms, respectively, and they were built intended in yielding 2D membranes with dimensions of about 100 × 100 Å², with periodic boundary conditions.

The equations of motion were solved using the velocity-Verlet integrator with a time-step of 0.1 fs. The tensile stress was considered in the system by applying a uniaxial strain along the periodic *x* and *y* directions, using an engineering strain rate of 10⁻⁵ fs⁻¹. The TMD membranes were stressed up to their complete rupture. To eliminate any residual stress within the membranes, they were equilibrated within an NPT ensemble at constant temperatures (1K and 300K) and null pressures using the Nosé-Hoover thermostat during 200 ps. By adopting this simulation protocol, Young's modulus (*Y*), Fracture Strain (*FS*), and Ultimate Strength (*US*) are the elastic properties derived from the stress-strain curves. The fracture dynamics, in turn, are studied through MD snapshots and the von Mises stress (VM) per-atom values, calculated at every 100 fs [49]. The VM values provide useful local structural information on the fracture mechanism, once they can determine the region from which the structure has started to yield the fractured lattice. The MD snapshots and trajectories were obtained by using free visualization and analysis software VMD [50].

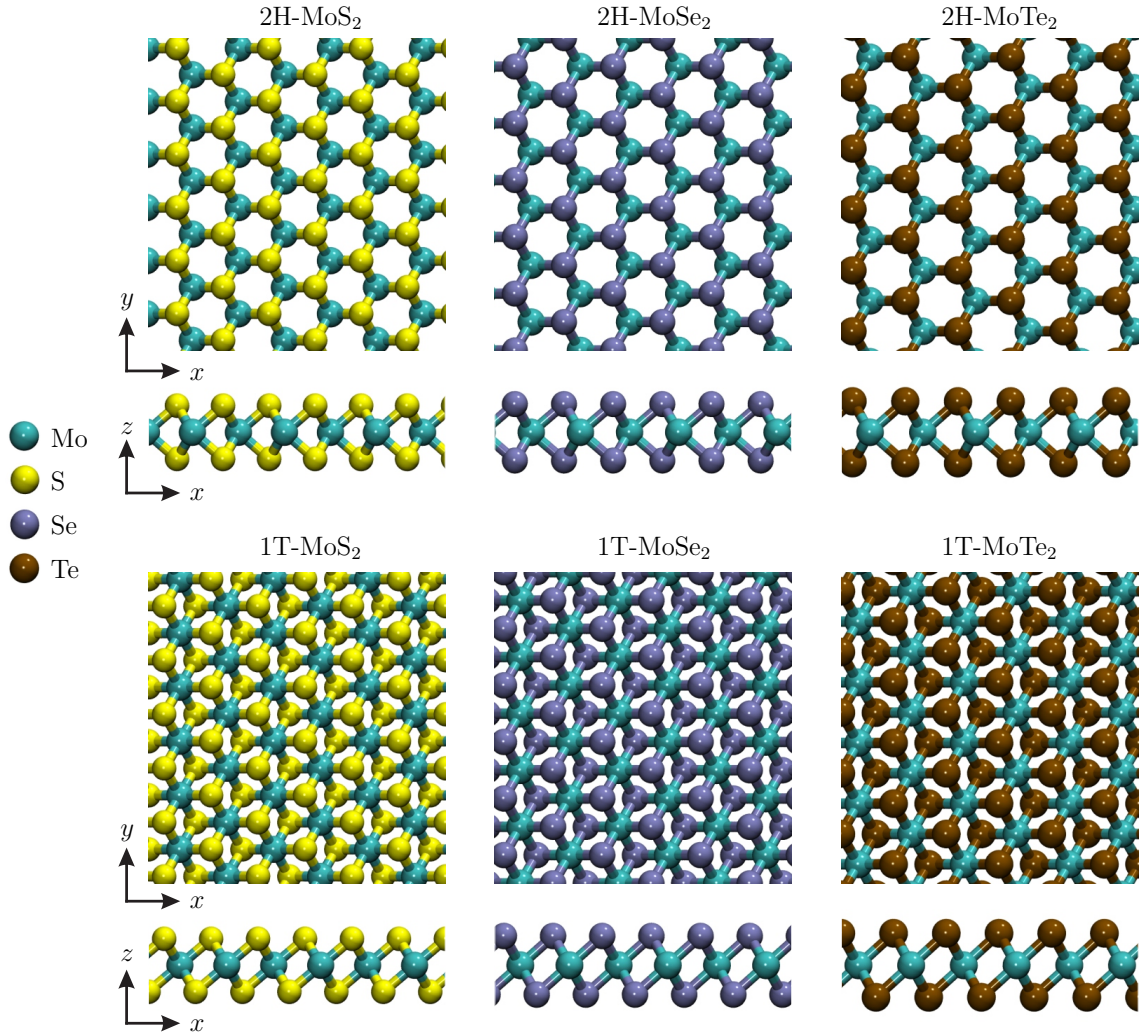


Figure 1: Schematic representation of the model TMDs monolayers in their 2H and 1T phases.

3. Results

We begin our discussions by showing representative MD snapshots of the fracture dynamics for the 2H-MoS₂ (top sequence of panels) and 1T-MoS₂ (bottom sequence of panels) monolayers at 300K and considering a uniaxial strain applied along the x -direction, as shown in Figure 2. In the 2H-MoS₂ case, one can note an abrupt rupture followed by a fast propagation of the fracture along the y – *direction* is accomplished at 11.60% of strain. The membrane is considered fractured at 11.68% of strain, once the atoms in the edges of the two fractures moieties are not interacting. A different fracture trend is realized for a 1T-MoS₂ membrane. The very first striking outcome obtained here, when contrasting the fracture dynamics of 2H-MoS₂ and 1T-MoS₂, is the considerably higher degree of fragility of the latter case. In Figure 2, one can observe that the critical strain for the beginning of the fracture in the 1T-MoS₂ (5.44%)

is almost two times smaller than the one for 2H- MoS_2 . Another clear trend showed in this figure is that the fracture dynamics of 1T- MoS_2 leads to a brittle lattice structure. This rupture trend is different from the one obtained for the 2H- MoS_2 case, in which two well concise MoS_2 fragments were produced as a final stage of the fracture process. This brittle signature for the 1T- MoS_2 case is obtained for 5.60% of strain. These results suggest that the translated arrangement of the chalcogen atoms in the 1T phase is crucial in diminishing the structural stability of TMDs.

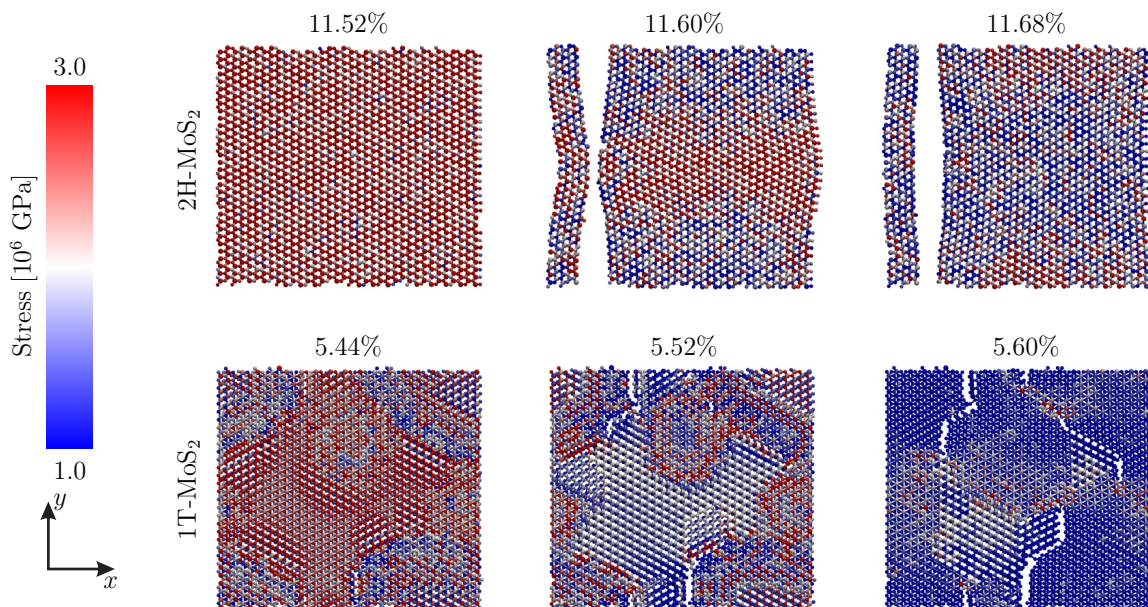


Figure 2: Representative MD snapshots of the fracture dynamics for the 2H- MoS_2 (top sequence of panels) and 1T- MoS_2 (bottom sequence of panels) monolayers at 300K and considering a uniaxial strain applied along the x -direction.

An interesting result arises when a uniaxial strain is applied along the y -direction, as depicted in Figure 3. This figure shows the cases related to Figure 2. When the tensile stretching is applied in the y -direction, the critical strain to realize the beginning of the fracture of 2H- MoS_2 and 1T- MoS_2 membranes is considerably higher than the ones presented in Figure 2). The difference between the fracture strains for these species is smaller when the stretching is applied along the y -direction. As illustrated in Figure 3, the fracture (critical) strains for the beginning of the rupture are 14.08% and 9.84% for the 2H- MoS_2 and 1T- MoS_2 membranes, respectively. After that critical value, the crack propagation takes place for 14.16% and 9.92% for the 2H- MoS_2 and 1T- MoS_2 cases, respectively. Interestingly, the brittle trend for the 1T- MoS_2 fracture, obtained for the y -direction stretching, not occurs when it comes to the y -direction stretching. After 14.24% and 10.0%, a fast crack propagation occurs for the 2H- MoS_2 and 1T- MoS_2 monolayers, respectively.

Figure 4 illustrates the representative MD snapshots for the 2H/1T- MoSe_2 and 2H/1T- MoTe_2 membranes. For the sake of convenience, we presented just the snapshots that show the crack propagation and the fractured form of

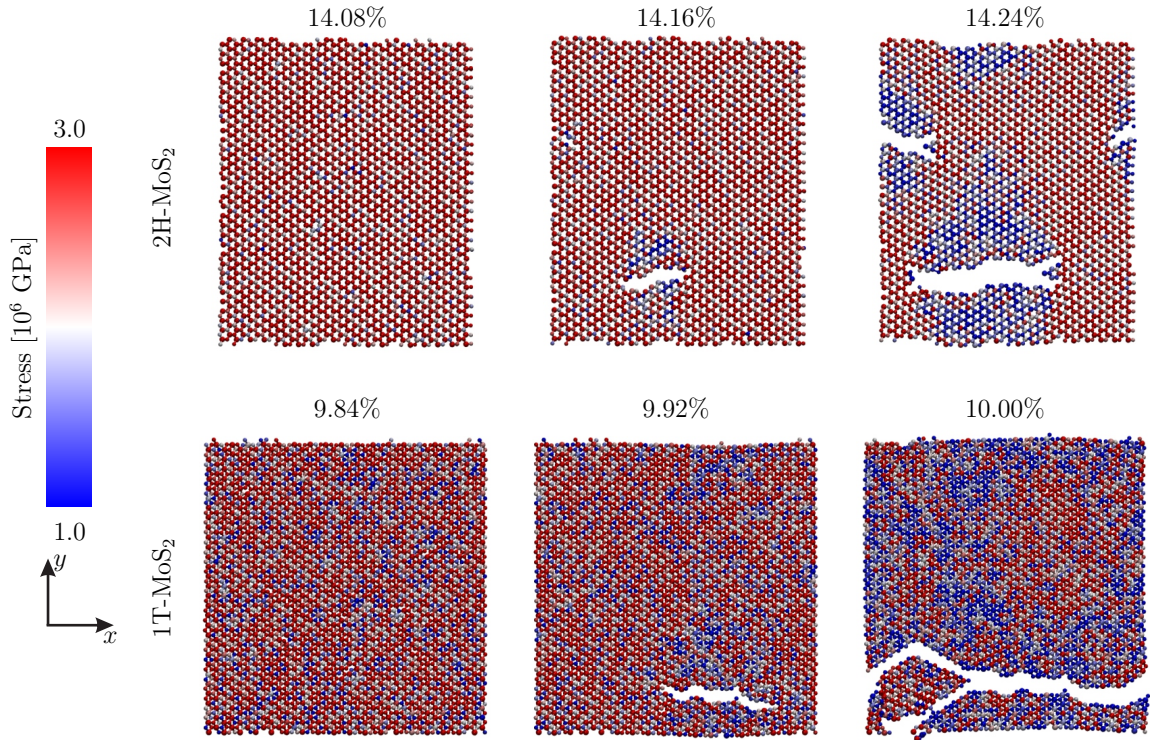


Figure 3: Representative MD snapshots of the fracture dynamics for the 1T-MoS₂ (top sequence of panels) and 1T-MoS₂ (bottom sequence of panels) monolayers at 300K and considering a uniaxial strain applied along the y -direction.

these TMD species. The top and bottom panels depict the results when the uniaxial strain is applied along the x and y directions, respectively. In the top panels, one can note that the critical strain for the membrane rupture is 17.60%, 7.52%, 18.56%, and, 8.24% for the 2H-MoSe₂, 1T-MoSe₂, 2H-MoTe₂, and 1T-MoTe₂, respectively. In the bottom panels, we can observe that the critical strain for the membrane rupture is 19.84%, 8.56%, 20.48%, and, 9.44% for the 2H-MoSe₂, 1T-MoSe₂, 2H-MoTe₂, and 1T-MoTe₂, respectively. A comparison of the tensile strength among the TMDs studied here is presented below with Table 1. As for the MoS₂ cases, in the MoSe₂ and MoTe₂ cases, the fracture propagation undergoes in the direction opposite to the stretching. It is worthwhile to stress that both MoSe₂ and MoTe₂ present a fracture mechanism defined by a fast crack propagation followed by an abrupt rupture of the membranes into parts with a good degree of integrity (i.e., no brittle structures were observed). These results suggest that MoSe₂ and MoTe₂ monolayers may present greater structural stability than the MoS₂ ones.

Finally, we present the elastic properties obtained from the simulations discussed above. These properties are Young's modulus (Y_M , in units of GPa), fracture strain ($FS(\%)$), and the maximum stress σ_{US} (which is called Ultimate Tensile Strength US (GPa)). They were estimated considering stretching regimes before mechanical failure (fracture) of the TMD membranes. These stretching regimes can be inferred from Figure 5, which illustrates the calculated

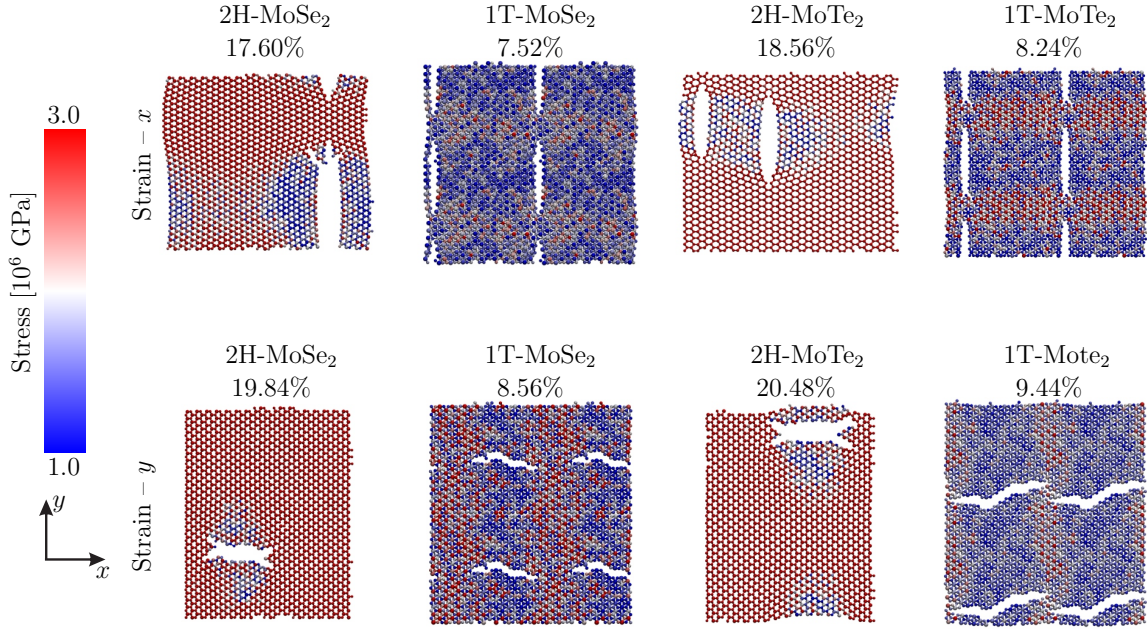


Figure 4: Representative MD snapshots of the fracture dynamics for the 2H/1T-MoSe₂ and 2H/1T-MoTe₂ monolayers at 300K. The top and bottom sequence of panels refer to the simulations considering a uniaxial strain applied along the x and y directions, respectively.

stress-strain curves for all TMD membranes when subjected to 10K and 300K, considering a uniaxial strain applied in both x and y directions. Figures 5(a-d), 5(b-e), and 5(c-f) are describing the stress-strain relationship for the 2H/1T-MoS₂, 2H/1T-MoSe₂, and 2H/1T-MoTe₂ membranes, respectively. Table 1 present a summary of the mechanical properties of the TMD monolayers studied in this work. In our simulation protocol, these monolayers were stretched at a constant rate until their total rupture. The stress-strain curves shown the two following common regions: a quasi-linear elastic region that is observed up to the ultimate strength value and a region of null stress (after a critical fracture strain) in which the TMD membranes ultimately break. In Figure 5, one can see that the US values are slightly higher for the cases in which the tensile stretching was applied in the y -direction. This trend occurs since the bond angle variations in x - and y -direction are different, and they govern the fracture strain. The fracture strains range from 5.44% (1T-MoS₂ at 300K) up to 29.86% (2H-MoTe₂ at 10K). As expected, increasing the temperature to 300K, there are a decrease in the critical tensile strain (fracture strain) values for all TMD membranes (see 1). The highest Young's Modulus was obtained for 2H-MoSe₂ monolayer at 10K (154.65 GPa). The TMD of the higher tensile strength (highest ultimate stress value) is the 2H-MoSe₂ membrane at 10K (25.98 GPa). As discussed above, generally, the translated arrangement of the chalcogen atoms in the 1T phase can contribute to diminishing their structural stability when compared with TMD membranes in the 2H phase. Importantly, Table 1 summarizes the elastic properties (Y_M , FS , and US) that were obtained by fitting the stress-strain curves for the TMD monolayers investigated here.

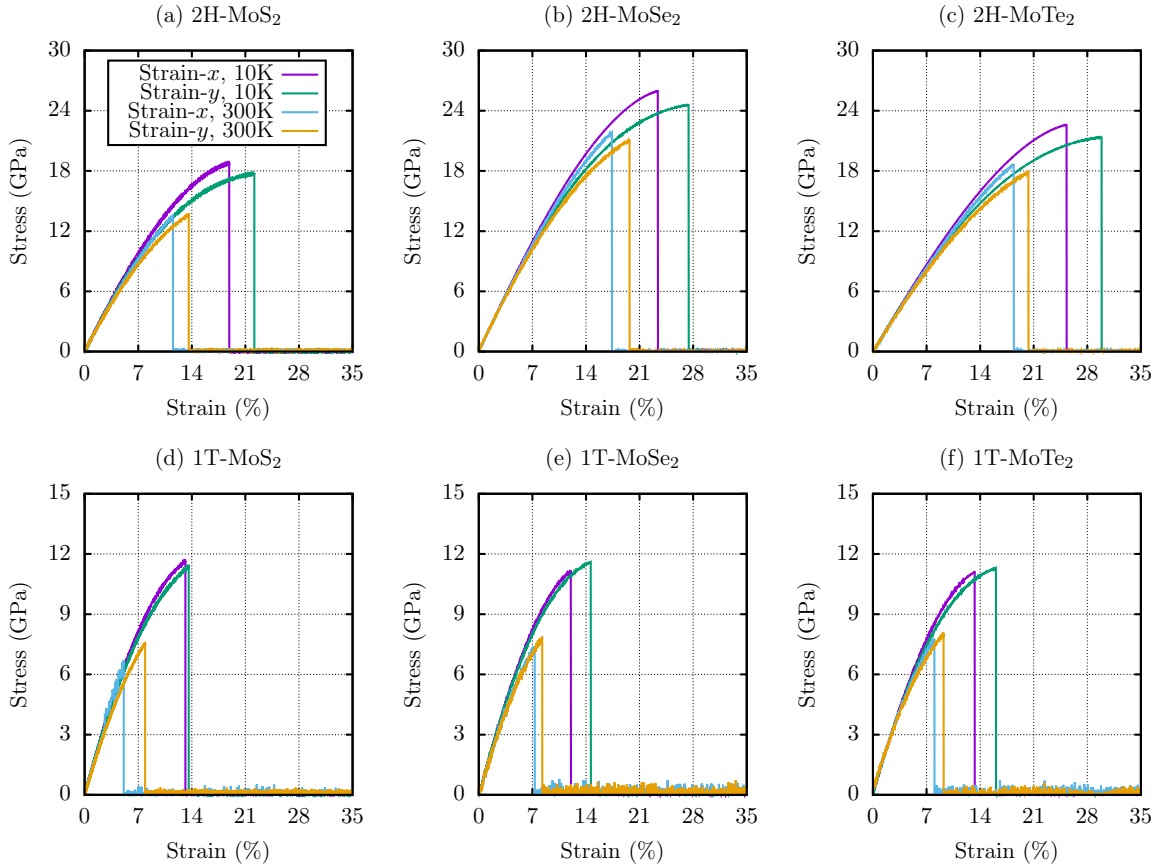


Figure 5: Calculated stress-strain curves for all TMD membranes studied here when subjected to 10K and 300K, considering a uniaxial strain applied in both x and y directions. Figures 5(a-d), 5(b-e), and 5(c-f) are describing the stress-strain relationship for the 2H/1T- MoS_2 , 2H/1T- MoSe_2 , and 2H/1T- MoTe_2 membranes, respectively.

4. Conclusions

In summary, we carried out fully-atomistic reactive molecular dynamics simulations to perform a comparative study on the elastic properties and fracture patterns of MoX_2 ($X=\text{S},\text{Se},\text{Te}$) membranes, in the 2H and 1T phases, within the framework of the Stillinger-Weber potential. The results showed that the fracture mechanism of a 2H- MoS_2 monolayer occurs through an abrupt rupture followed by fast crack propagation. A different fracture trend is realized for a 1T- MoS_2 membrane. The fracture dynamics of this material leads to a brittle structure. Both MoSe_2 and MoTe_2 presented a fracture mechanism defined by a fast crack propagation followed by an abrupt rupture of the membranes into parts with a good degree of integrity (i.e., no brittle structures were observed). These results suggest that these monolayers may present greater structural stability than the MoS_2 ones. The highest Young's Modulus has obtained for 2H- MoSe_2 monolayer at 10K (154.65 GPa). The TMD of higher tensile strength is the 2H- MoSe_2 membrane at 10K (25.98 GPa). Generally, the critical strain to realize the TMD membranes fracture is considerably higher when the

| 2H-MoS ₂ | | | | | | |
|----------------------|-------------|--------|----------|-------------|--------|----------|
| Temperature [K] | Strain-x | | | Strain-y | | |
| | Y_M [GPa] | FS [%] | US [GPa] | Y_M [GPa] | FS [%] | US [GPa] |
| 10 K | 144.92 | 18.89 | 18.81 | 139.43 | 22.16 | 17.76 |
| 300 K | 135.13 | 11.54 | 13.57 | 130.13 | 13.60 | 13.80 |
| 2H-MoSe ₂ | | | | | | |
| Temperature [K] | Strain-x | | | Strain-y | | |
| | Y_M [GPa] | FS [%] | US [GPa] | Y_M [GPa] | FS [%] | US [GPa] |
| 10 K | 159.63 | 23.39 | 25.98 | 154.65 | 27.41 | 24.59 |
| 300 K | 153.81 | 17.39 | 21.88 | 148.80 | 19.68 | 21.16 |
| 2H-MoTe ₂ | | | | | | |
| Temperature [K] | Strain-x | | | Strain-y | | |
| | Y_M [GPa] | FS [%] | US [GPa] | Y_M [GPa] | FS [%] | US [GPa] |
| 10 K | 125.21 | 25.29 | 22.61 | 121.54 | 29.86 | 21.37 |
| 300 K | 121.46 | 18.39 | 18.70 | 117.63 | 20.30 | 17.98 |
| 1T-MoS ₂ | | | | | | |
| Temperature [K] | Strain-x | | | Strain-y | | |
| | Y_M [GPa] | FS [%] | US [GPa] | Y_M [GPa] | FS [%] | US [GPa] |
| 10 K | 123.98 | 13.16 | 11.66 | 120.42 | 13.60 | 11.42 |
| 300 K | 132.65 | 5.11 | 6.91 | 110.00 | 7.90 | 7.62 |
| 1T-MoSe ₂ | | | | | | |
| Temperature [K] | Strain-x | | | Strain-y | | |
| | Y_M [GPa] | FS [%] | US [GPa] | Y_M [GPa] | FS [%] | US [GPa] |
| 10 K | 127.02 | 12.03 | 11.20 | 124.32 | 14.62 | 11.60 |
| 300 K | 114.41 | 7.31 | 7.70 | 111.80 | 8.28 | 8.02 |
| 1T-MoTe ₂ | | | | | | |
| Temperature [K] | Strain-x | | | Strain-y | | |
| | Y_M [GPa] | FS [%] | US [GPa] | Y_M [GPa] | FS [%] | US [GPa] |
| 10 K | 117.86 | 13.28 | 11.12 | 114.40 | 16.06 | 11.29 |
| 300 K | 107.16 | 8.03 | 7.91 | 103.02 | 9.23 | 8.19 |

Table 1

Elastic properties (Y_M , in units of GPa), fracture strain ($FS(\%)$), and the maximum stress σ_{US} (which is called Ultimate Tensile Strength US (GPa)) that were obtained by fitting the stress-strain curves for the TMD monolayers investigated here.

strain was applied along the y -direction. It was also obtained here as a general trend that the translated arrangement of the chalcogen atoms in the 1T phase can contribute to diminishing their structural stability when compared with TMD membranes in the 2H phase. As a consequence, among the 2H and 1T phases, the 1T presented lower tensile strength.

Acknowledgements

The authors gratefully acknowledge the financial support from Brazilian research agencies CNPq, FAPESP, and FAP-DF. M.L.P.J. gratefully acknowledge the financial support from CAPES grant 88882.383674/2019-01. R.T.S.J. gratefully acknowledge, respectively, the financial support from CNPq grants 465741/2014-2 and 312180/2019-5, CAPES grant 88887.144009/2017-00, and FAP-DF grants 0193.001366/2016 and 0193.001365/2016. L.A.R.J. acknowledges the financial support from a Brazilian Research Council FAP-DF and CNPq grants 00193.0000248/2019-32 and 302236/2018 – 0, respectively. L.A.R.J. and M.L.P.J. acknowledge CENAPAD-SP for providing the compu-

tational facilities.

References

- [1] Sajede Manzeli, Dmitry Ovchinnikov, Diego Pasquier, Oleg V Yazyev, and Andras Kis. 2d transition metal dichalcogenides. *Nature Reviews Materials*, 2(8):17033, 2017.
- [2] Manish Chhowalla, Hyeon Suk Shin, Goki Eda, Lain-Jong Li, Kian Ping Loh, and Hua Zhang. The chemistry of two-dimensional layered transition metal dichalcogenide nanosheets. *Nature chemistry*, 5(4):263–275, 2013.
- [3] Chaoliang Tan and Hua Zhang. Two-dimensional transition metal dichalcogenide nanosheet-based composites. *Chemical Society Reviews*, 44(9):2713–2731, 2015.
- [4] Manish Chhowalla, Zhongfan Liu, and Hua Zhang. Two-dimensional transition metal dichalcogenide (tmd) nanosheets. *Chemical Society Reviews*, 44(9):2584–2586, 2015.
- [5] Mingsheng Xu, Tao Liang, Minmin Shi, and Hongzheng Chen. Graphene-like two-dimensional materials. *Chemical reviews*, 113(5):3766–3798, 2013.
- [6] Sheneve Z Butler, Shawna M Hollen, Linyou Cao, Yi Cui, Jay A Gupta, Humberto R Gutiérrez, Tony F Heinz, Seung Sae Hong, Jiaying Huang, Ariel F Ismach, et al. Progress, challenges, and opportunities in two-dimensional materials beyond graphene. *ACS nano*, 7(4):2898–2926, 2013.
- [7] Xiaoxin Qian, Sida Shen, Teng Liu, Liang Cheng, and Zhuang Liu. Two-dimensional tis 2 nanosheets for in vivo photoacoustic imaging and photothermal cancer therapy. *Nanoscale*, 7(14):6380–6387, 2015.
- [8] Yu Chen, Chaoliang Tan, Hua Zhang, and Lianzhou Wang. Two-dimensional graphene analogues for biomedical applications. *Chemical Society Reviews*, 44(9):2681–2701, 2015.
- [9] Qing Hua Wang, Kouros Kalantar-Zadeh, Andras Kis, Jonathan N Coleman, and Michael S Strano. Electronics and optoelectronics of two-dimensional transition metal dichalcogenides. *Nature nanotechnology*, 7(11):699–712, 2012.
- [10] JI A Wilson and AD Yoffe. The transition metal dichalcogenides discussion and interpretation of the observed optical, electrical and structural properties. *Advances in Physics*, 18(73):193–335, 1969.
- [11] Goki Eda, Hisato Yamaguchi, Damien Voiry, Takeshi Fujita, Mingwei Chen, and Manish Chhowalla. Photoluminescence from chemically exfoliated mos2. *Nano letters*, 11(12):5111–5116, 2011.
- [12] Qinbai Yun, Qipeng Lu, Xiao Zhang, Chaoliang Tan, and Hua Zhang. Three-dimensional architectures constructed from transition-metal dichalcogenide nanomaterials for electrochemical energy storage and conversion. *Angewandte Chemie International Edition*, 57(3):626–646, 2018.
- [13] Kin Fai Mak, Changgu Lee, James Hone, Jie Shan, and Tony F Heinz. Atomically thin mos2: a new direct-gap semiconductor. *Physical review letters*, 105(13):136805, 2010.
- [14] Claudia Ruppert, Ozgur Burak Aslan, and Tony F Heinz. Optical properties and band gap of single-and few-layer mote2 crystals. *Nano letters*, 14(11):6231–6236, 2014.
- [15] Deep Jariwala, Vinod K Sangwan, Lincoln J Lauhon, Tobin J Marks, and Mark C Hersam. Emerging device applications for semiconducting two-dimensional transition metal dichalcogenides. *ACS nano*, 8(2):1102–1120, 2014.
- [16] Yi Zhang, Tay-Rong Chang, Bo Zhou, Yong-Tao Cui, Hao Yan, Zhongkai Liu, Felix Schmitt, James Lee, Rob Moore, Yulin Chen, et al. Direct observation of the transition from indirect to direct bandgap in atomically thin epitaxial mose2. *Nature nanotechnology*, 9(2):111, 2014.
- [17] Ali Eftekhari. Molybdenum diselenide (mose2) for energy storage, catalysis, and optoelectronics. *Applied Materials Today*, 8:1–17, 2017.

- [18] Goki Eda and Stefan A Maier. Two-dimensional crystals: managing light for optoelectronics. *ACS nano*, 7(7):5660–5665, 2013.
- [19] Xiao Zhang, Zhuangchai Lai, Qinglang Ma, and Hua Zhang. Novel structured transition metal dichalcogenide nanosheets. *Chemical Society Reviews*, 47(9):3301–3338, 2018.
- [20] Alireza Ostadhossein, Ali Rahnamoun, Yuanxi Wang, Peng Zhao, Sulin Zhang, Vincent H Crespi, and Adri CT Van Duin. Reaxff reactive force-field study of molybdenum disulfide (mos_2). *The journal of physical chemistry letters*, 8(3):631–640, 2017.
- [21] Andres Castellanos-Gomez, Menno Poot, Gary A Steele, Herre SJ Van Der Zant, Nicolás Agraït, and Gabino Rubio-Bollinger. Elastic properties of freely suspended mos_2 nanosheets. *Advanced materials*, 24(6):772–775, 2012.
- [22] Andres Castellanos-Gomez, Ronald van Leeuwen, Michele Buscema, Herre SJ van der Zant, Gary A Steele, and Warner J Venstra. Single-layer mos_2 mechanical resonators. *Advanced Materials*, 25(46):6719–6723, 2013.
- [23] Andres Castellanos-Gomez, Rafael Roldán, Emmanuele Cappelluti, Michele Buscema, Francisco Guinea, Herre SJ van der Zant, and Gary A Steele. Local strain engineering in atomically thin mos_2 . *Nano letters*, 13(11):5361–5366, 2013.
- [24] Ryan C Cooper, Changgu Lee, Chris A Marianetti, Xiaoding Wei, James Hone, and Jeffrey W Kysar. Nonlinear elastic behavior of two-dimensional molybdenum disulfide. *Physical Review B*, 87(3):035423, 2013.
- [25] Jin-Wu Jiang and Harold S Park. Mechanical properties of mos_2 /graphene heterostructures. *Applied Physics Letters*, 105(3):033108, 2014.
- [26] Jin-Wu Jiang, Harold S Park, and Timon Rabczuk. Molecular dynamics simulations of single-layer molybdenum disulfide (mos_2): Stillinger-weber parametrization, mechanical properties, and thermal conductivity. *Journal of Applied Physics*, 114(6):064307, 2013.
- [27] Jun Kang, Hasan Sahin, and François M Peeters. Mechanical properties of monolayer sulphides: a comparative study between mos_2 , hfs_2 and tis_3 . *Physical Chemistry Chemical Physics*, 17(41):27742–27749, 2015.
- [28] Muhammad Bilal Khan, Rahim Jan, Amir Habib, and Ahmad Nawaz Khan. Evaluating mechanical properties of few layers mos_2 nanosheets-polymer composites. *Advances in Materials Science and Engineering*, 2017, 2017.
- [29] Tao Liang, Simon R Phillpot, and Susan B Sinnott. Parametrization of a reactive many-body potential for mo-s systems. *Physical Review B*, 79(24):245110, 2009.
- [30] Kai Liu, Qimin Yan, Michelle Chen, Wen Fan, Yinghui Sun, Joonki Suh, Deyi Fu, Sangwook Lee, Jian Zhou, Sefaattin Tongay, et al. Elastic properties of chemical-vapor-deposited monolayer mos_2 , ws_2 , and their bilayer heterostructures. *Nano letters*, 14(9):5097–5103, 2014.
- [31] Sajedeheh Manzeli, Adrien Allain, Amirhossein Ghadimi, and Andras Kis. Piezoresistivity and strain-induced band gap tuning in atomically thin mos_2 . *Nano letters*, 15(8):5330–5335, 2015.
- [32] Oleg V Yazyev and Andras Kis. Mos_2 and semiconductors in the flatland. *Materials Today*, 18(1):20–30, 2015.
- [33] Bohayra Mortazavi, Alireza Ostadhossein, Timon Rabczuk, and Adri CT Van Duin. Mechanical response of all- mos_2 single-layer heterostructures: a reaxff investigation. *Physical Chemistry Chemical Physics*, 18(34):23695–23701, 2016.
- [34] Pere Miró, Mahdi Ghorbani-Asl, and Thomas Heine. Two dimensional materials beyond mos_2 : noble-transition-metal dichalcogenides. *Angewandte Chemie International Edition*, 53(11):3015–3018, 2014.
- [35] Riccardo Frisenda, Matthias Drüppel, Robert Schmidt, Steffen Michaelis de Vasconcellos, David Perez de Lara, Rudolf Bratschitsch, Michael Rohlfing, and Andres Castellanos-Gomez. Biaxial strain tuning of the optical properties of single-layer transition metal dichalcogenides. *npj 2D Materials and Applications*, 1(1):1–7, 2017.
- [36] Y. M. Jaques, P. Manimunda, Y. Nakanishi, S. Susarla, C. F. Woellner, S. Bhowmick, S. A. S. Asif, D. S. Galvão, C. S. Tiwary, P. M. Ajayan, and et al. Differences in the mechanical properties of monolayer and multilayer $\text{wse}_2/\text{mose}_2$. *MRS Advances*, 3(6-7):373–378, 2018.
- [37] Miao Jiang, Junjun Zhang, Meihui Wu, Wenjing Jian, Hongtao Xue, Tsz-Wai Ng, Chun-Sing Lee, and Jun Xu. Synthesis of 1t- mose_2 ultrathin nanosheets with an expanded interlayer spacing of 1.17 nm for efficient hydrogen evolution reaction. *Journal of Materials Chemistry*

Mechanical Properties of MoX₂ (X = S, Se, Te) Membranes

- A, 4(39):14949–14953, 2016.
- [38] Nestor Iguiñiz, Riccardo Frisenda, Rudolf Bratschitsch, and Andres Castellanos-Gomez. Revisiting the buckling metrology method to determine the young's modulus of 2d materials. *Advanced Materials*, 31(10):1807150, 2019.
- [39] Priya Johari and Vivek B Shenoy. Tuning the electronic properties of semiconducting transition metal dichalcogenides by applying mechanical strains. *ACS nano*, 6(6):5449–5456, 2012.
- [40] Ashok Kumar and PK Ahluwalia. Mechanical strain dependent electronic and dielectric properties of two-dimensional honeycomb structures of mox₂ (x= s, se, te). *Physica B: Condensed Matter*, 419:66–75, 2013.
- [41] Bohayra Mortazavi, Golibjon R Berdiyrov, Meysam Makaremi, and Timon Rabczuk. Mechanical responses of two-dimensional mote₂; pristine 2h, 1t and 1t' and 1t'/2h heterostructure. *Extreme Mechanics Letters*, 20:65–72, 2018.
- [42] Claudia Ruppert, Ozgur Burak Aslan, and Tony F Heinz. Optical properties and band gap of single-and few-layer mote₂ crystals. *Nano letters*, 14(11):6231–6236, 2014.
- [43] Peter May, Umar Khan, and Jonathan N Coleman. Reinforcement of metal with liquid-exfoliated inorganic nano-platelets. *Applied Physics Letters*, 103(16):163106, 2013.
- [44] B Rahman Rano, Ishtiaque M Syed, and SH Naqib. Ab initio approach to the elastic, electronic, and optical properties of mote₂ topological weyl semimetal. *Journal of Alloys and Compounds*, page 154522, 2020.
- [45] Yufei Sun, Jinbo Pan, Zetao Zhang, Kenan Zhang, Jing Liang, Weijun Wang, Zhiquan Yuan, Yukun Hao, Bolun Wang, Jingwei Wang, et al. Elastic properties and fracture behaviors of biaxially deformed, polymorphic mote₂. *Nano letters*, 19(2):761–769, 2019.
- [46] Shuo Deng, Lijie Li, and Min Li. Stability of direct band gap under mechanical strains for monolayer mos₂, mose₂, ws₂ and wse₂. *Physica E: Low-dimensional Systems and Nanostructures*, 101:44 – 49, 2018.
- [47] Nestor Iguiñiz, Riccardo Frisenda, Rudolf Bratschitsch, and Andres Castellanos-Gomez. Revisiting the buckling metrology method to determine the young's modulus of 2d materials. *Advanced Materials*, 31(10):1807150, 2019.
- [48] Steve Plimpton. Fast parallel algorithms for short-range molecular dynamics. *Journal of computational physics*, 117(1):1–19, 1995.
- [49] Marcelo Lopes Pereira and Luiz Antônio Ribeiro. Thermomechanical insight into the stability of nanoporous graphene membranes. *FlatChem*, 24:100196, 2020.
- [50] William Humphrey, Andrew Dalke, and Klaus Schulten. Vmd: Visual molecular dynamics. *Journal of Molecular Graphics*, 14(1):33 – 38, 1996.